The Influence of Specular Reflections on Bistatic Tropospheric Radio Scatter from Turbulent Strata[1]

DAVID ATLAS, R. C. SRIVASTAVA AND W. S. MARKER, JR.

Dept. of the Geophysical Sciences, The University of Chicago

(Manuscript received 17 March 1969, in revised form 26 June 1969)

ABSTRACT

Specular reflection from a stratum of sharp, mean, vertical refractivity gradient frequently accompanies the scatter from the turbulent perturbations in refractivity which tend to be maximized close to the gradient. As a result, the signal intensity falls more rapidly, and the magnitude of the mean Doppler shift increases less rapidly with beam offset angle from the great circle than is the case for pure turbulent scatter. Also, in transmission via the great circle path, the Doppler spread, signal fading rate, and multi-path spread may be greatly reduced from that expected for turbulent scatter alone. Because transmission along the great circle may be greatly influenced by specular reflections, the strength of which is a function of the form and sharpness of the mean refractivity gradient, past experiments relating signal-wavelength dependence or signal-scatter angle dependence to the form of the turbulent refractivity spectrum are suspect.

1. Introduction

Birkemeier *et al.* (1968) and Atlas *et al.* (1969) have discussed the measurement of the velocity of refractively perturbed atmospheric layers by means of bistatic Doppler beam-swinging experiments. The beams are swung synchronously and the time-rate of phase shift in two-way transmission between the antennas is measured as a function of the beam offset from the great circle. The referenced papers deal only with a model which assumes scatter from a thin refractively turbulent layer. Here we are concerned with the effects on the measurements resulting from the simultaneous presence of a specularly reflecting stratum.

2. The problem

Details of the Doppler beam-swinging experiments may be found in the above-referenced papers. In both papers the authors have interpreted the Doppler frequency shift experiment in terms of the cross-beam motion of the scatterers or "blobs" in a single dominant scattering layer. For small offset angles from the great circle, the Doppler shift is proportional to the speed of the scatterers and to their perpendicular distance from great circle (see Fig. 1) or $f=cvy$, where c is a constant. As a result, it was shown by Atlas *et al.* that the Doppler spectrum of the scattered signal is an image of the distribution of signal power with y, or $S(f)df=P(y)dy$. One may then expect the mean frequency shift to be proportional to the antenna offset distance Y. However, from Atlas *et al.*, the reflectivity η_i of the scattering layer varies as

$$\eta_i(y,z)=\eta_i(0,z)\left(\frac{z^2}{z^2+y^2}\right)^{p/2}, \tag{1}$$

where $\eta_i(0,z)$ is the reflectivity at $y=0$, and p is a parameter which is equal to $\nu+2$, ν being the exponent in the one-dimensional spectrum $F(k)$ of refractivity vs wavenumber, such that $F(k)\propto k^{-\nu}$. In (1), the x dependence of reflectivity has not been considered. As shown by Atlas *et al.* for the case of a vertically thin scatter layer at height z, the decrease of reflectivity with y causes the Doppler frequency shift to be proportional to $\hat{y}$ where $|\hat{y}|<|Y|$, $\hat{y}$ being the y at which $P(y)$ is a maximum. In other words, since the signal spectrum $P(y)$ is a product of the beam illumination pattern centered at $|Y|$ with the reflectivity function (1), the maxi-

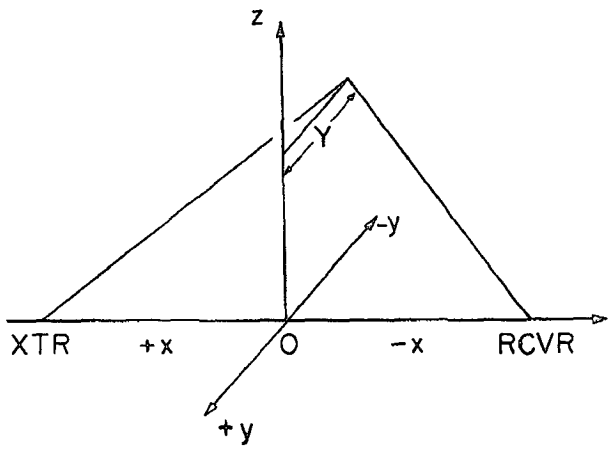

FIG. 1. Schematic diagram showing the experimental arrangement.

[1] Research supported in part by the National Science Foundation under Grant GA-819 and by a grant from the United Airlines Foundation.

mum of $P(y)$ will always be found on the high reflectivity side of the beam axis. Because $\eta_t(y,z)$ has a maximum on the great circle at $y=0$, the maximum of $P(y)$ and its mean will always occur on the great circle side of the beam axis.

The general form of y is shown by curve B in Fig. 2, with some of the curves of Doppler shift observed by Birkemeier *et al.* being shown in Fig. 3. While these Fig. 3 experimental curves generally resemble curve B of Fig. 2, they are sometimes found to depart considerably from it when the frequency shift scale is converted to a distance scale, i.e., $\bar{y}=f/(cv)$. The curves are then found to be closer to C (Fig. 2), so that the Doppler frequency shift remains nearly zero for considerable antenna offsets. In this paper, it is suggested that this feature of the observations is due to the presence of specularly reflected components in the transmitted

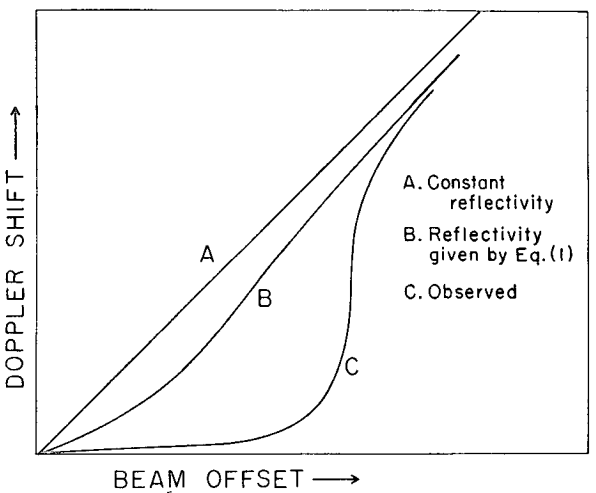

FIG. 2. Schematic diagram showing the Doppler shift vs antenna beam offset for constant reflectivity, A; reflectivity for turbulent layer, B, from Eq. (1); observed, C.

signal. It will be assumed that the layer responsible for the specular reflection is plane and horizontal. Consequently, the specularly reflected signal will come only from near the great circle, and the associated Doppler frequency shift will be zero. It should be remembered, however, that in nature, such layers may very well be somewhat tilted and undulative, so that specular reflections may arise also from points not near the great circle.

3. Computations and discussion

Let η_s denote the specular component of the reflectivity, so that the total reflectivity is $(\eta_s+\eta_t)$, where η_t is the turbulent reflectivity as given by (1). Since the Doppler shift is proportional to y, the mean of the Doppler power spectrum as a function of antenna offset

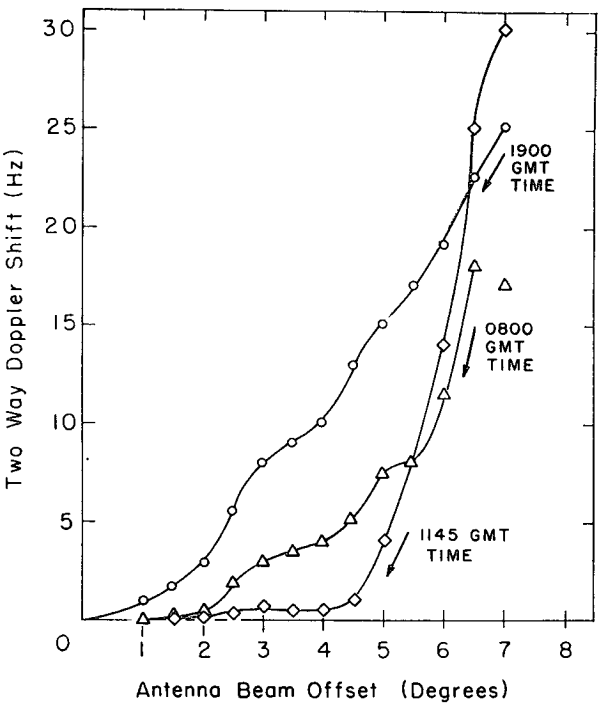

FIG. 3. Two-way Doppler shift vs antenna beam offset observed on the Arlington, Wisconsin-Cedar Rapids link.

distance Y is given by

$$\bar{y}(Y)=\int_{-\infty}^{+\infty} y(\eta_s+\eta_t)I(y,Y)dy \Big/ \int_{-\infty}^{+\infty}(\eta_s+\eta_t)I(y,Y)dy, \quad (2)$$

where $I(y,Y)$ denotes the two-way antenna illumination pattern when it is offset at a distance Y from the great circle at midpath. Following Atlas *et al.*, we ignore the x dependence of the antenna illumination pattern, so that

$$I(y,Y)=I_0\exp\left[-2\left(\frac{y-Y}{y_0}\right)^2\right], \quad (3)$$

y_0 being related to the beam widths of the antennas. The denominator in (2) is proportional to the total power. It should be noted in contrast to Atlas *et al.*, who use the peak $\hat{y}$ of the Doppler power spectrum, that we have used in (2) the average $\bar{y}$ of the spectrum. However, as shown by Atlas *et al.*, the difference between $\hat{y}$ and $\bar{y}$ decreases with increasing height of the scattering layer, and may be neglected when this height exceeds ~3–4 km. Now, if the reflecting layer is plane and horizontal, the specularly reflected signal is received only from near the great circle; as an idealization, we assume $\eta_s=0$, if $y\neq 0$. Hence,

$$\int_{-\infty}^{+\infty}\eta_s I(y,Y)dy=I(0,Y)\int_{-\infty}^{+\infty}\eta_s dy. \quad (4)$$

Thus, η_s behaves like a δ function, being non-zero only at $y=0$, but enclosing a finite area. The integral on the right-hand side is a measure of the strength of the specular reflection. As a measure of this strength, let us define a factor F as

$$F=\int_{-\infty}^{+\infty}\eta_s dy \Big/ \eta_t(0,z). \tag{5}$$

Obviously, F has the dimensions of a length. With the help of (4) and (5), Eq. (1) may then be written as

$$\bar{y}(Y)=\int_{-\infty}^{+\infty} y\eta_t^* I(y,Y)dy \Big/\left[\int_{-\infty}^{+\infty}\eta_t^* I(y,Y)dy+F\cdot I(0,Y)\right], \tag{6}$$

where η_t^* is the turbulent reflectivity normalized by $\eta(0,z)$, i.e.,

$$\eta_t^*=\left(\frac{z^2}{y^2+z^2}\right)^{p/2}. \tag{7}$$

Recalling that $f=cvy$, then $\bar{y}=\bar{f}/(cv)$ may be regarded as the normalized average of the Doppler power spectrum. Computations of the Doppler shift $\bar{y}$, according to (6), and the 'normalized' power as measured by the denominator in (6), have been performed for various values of F and other parameters corresponding to the Wisconsin bistatic radio link[2]. Some of the results are shown in Figs. 4 and 5. Fig. 4 shows, with specular reflection, that the Doppler shift remains nearly zero for considerable antenna offsets. As expected, this effect increases as the strength of the specular reflection F is increased. Thus, the assumption of specular reflection helps to explain this feature of the observations.

Another observation, which may help to decide whether or not specular reflection is present, is the variation of total power with antenna offset distance. The computed variation is shown in Fig. 5 for the same cases as in Fig. 4. It is seen with turbulent scatter only ($F=0$), that the power falls off comparatively less sharply with antenna offset distance Y. As the strength of specular reflection increases, the curve becomes more steep, and approaches the two-way illumination pattern of the antennas as shown by the curve for $F=1024$ km in Fig. 5. In this case, of course, since the strong specular reflection at $y=0$ acts as a point scatterer, beam swinging across it reproduces the combined antenna pattern.

Obviously, another consequence of strong specular layers will be a narrow Doppler spectrum and associated slow signal fading rate, i.e., the signal fading rate spectrum has a variance twice that of the Doppler spectrum. Clearly, such strong specular reflections will also be accompanied by a narrow multi-path spread since the received signal is due mainly to the component transmitted along the great circle and only negligibly to scatter via turbulent eddies off the great circle, for which the time of propagation is greater.

It is of interest to compare the experimental data of Fig. 3 to the corresponding theoretical curves of Fig. 4.

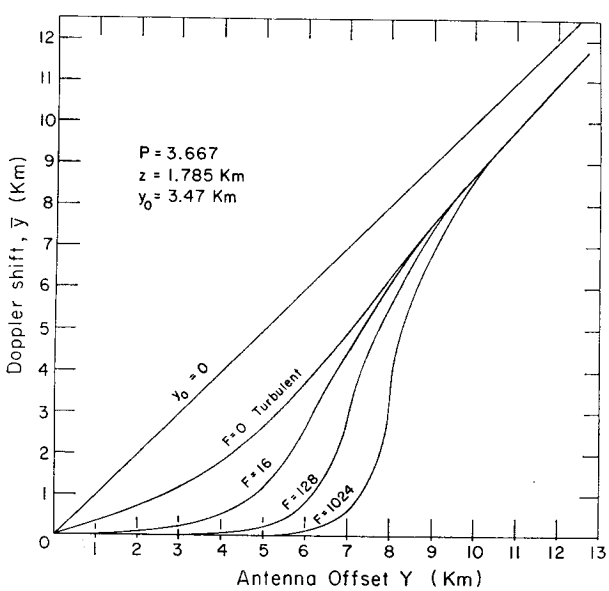

FIG. 4. Mean Doppler shift vs antenna offset for infinitely narrow beam ($y_0=0$), one turbulent layer ($F=0$), and combinations of one turbulent layer and various strengths (F, km) of specular reflection.

[2] See Atlas *et al.* (1969) for the link characteristics.

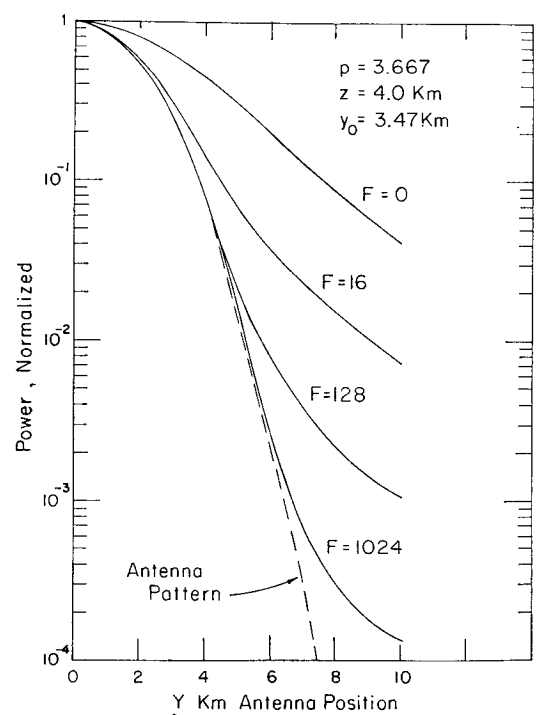

FIG. 5. Computed variation of normalized power with antenna position for a turbulent layer ($F=0$), and combination of a turbulent layer with various strengths of specular reflection (F, km). The dashed curve shows the antenna pattern when the offset $Y=0$.

The diurnal variation of the mean Doppler shift curves in Fig. 3 is especially significant. We see that the 1900 GMT (mid-afternoon in Madison, Wis.) appear to behave more or less in accordance with the theory of Atlas *et al.* for a thin turbulent scatter layer. During the middle of the night (0800 GMT), however, as the atmospheric stability increases, $\bar{f}$ remains close to zero out to a beam offset angle of 2°. Finally, in the early morning (1145 GMT), with the strength of the nocturnal inversion near its maximum, there appears to be a very strong specular reflection which holds $\bar{f}$ near zero out to 4° offset angle. Clearly, the form of the 0800 and 1145 GMT curves is similar in its major features to those in Fig. 4. Note, however, that the Doppler shifts ultimately increase when the beams are skewed sufficiently to one side of the great circle. This is sufficient proof that turbulent scatter is indeed present even under what appear to be extremely stable conditions. One should therefore not be deceived that turbulent scatter is inoperative when his observations are restricted to pointing along the great circle. Indeed, we suggest that turbulent scatter is probably present most of the time at strata of sharp reflectivity gradients. That this is so is evidenced by the radar backscatter data of Hardy *et al.* (1966) which show fine echo layers at oblique incidence in association with inversions. Also, Lane (1968) has demonstrated that major perturbations in refractivity are indeed associated with sharp mean vertical gradients of refractivity. In the forward-scatter direction, both specular and turbulent scatter may occur essentially simultaneously; in the backscatter direction, of course, only the turbulent scatter is detectable.

For these reasons, we should now be suspicious of past tropo-scatter experiments made only along the great circle. In particular, Bolgiano's (1964) simultaneous measurements of signal power in scatter experiments at 3.2, 10.7 and 35.7 cm wavelengths aimed at deducing the wavenumber dependence of the refractivity spectrum probably included many cases of specular reflection. The dependence of signal strength on wavelength in such cases is a function of the form and sharpness of the mean reflectivity gradient, and large variations in this dependence are possible. Accordingly, if due to specular reflections, the associated dependence of signal power on wavelength has nothing whatsoever to do with the form of the turbulent refractivity spectrum. Recently, Bull and Neisser (1969) made measurements at two wavelengths, 3.2 and 12.5 cm. In the afternoons and in summer, they find the exponent ν in the one-dimensional refractivity spectrum to be about 3.5 at both wavelengths. However, in the morning and in winter, they find the exponent to be about 4.0 at the longer wavelength. This increase is attributable to the simultaneous occurrence of specular reflections, which are more likely at the longer wavelengths, and in the morning and winter when atmospheric stratifications are more frequent.

4. Conclusions

Strong specular reflections from a stratum of sharp mean vertical refractivity gradient frequently accompany the scatter associated with the turbulent perturbations in refractivity which tend to be maximized in the immediate vicinity of the gradient. The presence of such specular signal components has the following effects. In horizontal beam swinging experiments, the signal power falls more sharply with the beam offset angle from the great circle than is the case for pure turbulent scatter; and the magnitude of the mean Doppler shift increases less rapidly with beam offset than expected for turbulent scatter alone. This is to say that the signal and its Doppler spectrum may be weighted strongly by the specular components received via the great circle path even when the beam axes are skewed from that path. In transmission along the great circle, the variance of the Doppler spectrum, which is normally associated with the cross-beam velocity of the turbulent eddies, may be sharply reduced by the presence of strong specular reflections. In the case of phase-incoherent transmission, this is manifested by a reduced signal fading rate. Similarly, the multi-path spread is also reduced.

Because bistatic scatter with beams oriented along the great circle may be heavily influenced by specular reflections, and since the wavelength dependence of the specular component is a function of the shape and gradient of the mean vertical refractivity gradient, past experiments purporting to deduce the form of the turbulent refractivity spectrum either from the signal-wavelength dependence or the dependence on scatter angle are subject to serious doubt.

Acknowledgments. We are greatly indebted to Profs. W. P. Birkemeier and D. H. Sargeant of the University of Wisconsin for furnishing the experimental data and for stimulating discussions on the general subject.

REFERENCES

Atlas, D., R. C. Srivastava, R. E. Carbone and Sargeant 1969: Doppler crosswind relations in radio tropo-scatter beam swinging for a thin scatter layer. *J. Atmos. Sci.*, **26**, 1104–1117.

Birkemeier, W. P., H. S. Merrill, D. H. Sargeant, D. W. Thomson, C. M. Beamer and G. T. Bergemann, 1968: Observation of wind-produced Doppler shifts in tropospheric scatter propagation. *Radio Sci.*, **3**, 309–317.

Bolgiano, R., Jr., 1964: A study of wavelength dependence of trans-horizon propagation. Res. Rept. CRSR 188, Center of Radio Physics and Space Research, Cornell University, Ithaca, N. Y., 67 pp.

Bull, G., and J. Neisser, 1969: Investigation of the radio refractive index spectrum by radio propagation methods and microwave refractometer. *Radio Sci.*, **4** (in press).

Hardy, K. R., D. Atlas and K. M. Glover, 1966: Multiwavelength backscatter from the clear atmosphere. *J. Geophys. Res.*, **71**, 1537–1552.

Lane, J. A., 1968: Small-scale variations of radio refractive index in the troposphere. *Proc. Inst. Elec. Engrs., London*, **115**, 1227–1234.